ACS APPLIED MATERIALS & INTERFACES

Research Article

www.acsami.org

Tuning Physical and Optical Properties of ZnO Nanowire Arrays Grown on Cotton Fibers

Thushara J. Athauda,[†] Parameswar Hari,[‡] and Ruya R. Ozer*[,†]

[†]Department of Chemistry and Biochemistry, [‡]Department of Physics and Engineering Physics, University of Tulsa, Tulsa, Oklahoma 74104, United States

Supporting Information

ABSTRACT: This article reports the first systematic study on the quantitative relationship between the process parameters of solution concentration ratio, structure, and physical and optical properties of ZnO nanowires grown on cotton surfaces. To develop a fundamental understanding concerning the process−structure−activity relations, we grew a series of well-defined, radially oriented, highly dense, and uniform single-crystalline ZnO nanorods and nanoneedles on cotton surfaces by a simple and inexpensive two-step optimized hydrothermal process at a relatively low temperature. This process involves seed treatment of a cotton substrate with ZnO nanocrystals that will serve as the nucleation sites for subsequent anisotropic growth of single crystalline ZnO nanowires. All of the ZnO nanowires exhibit wurtzite crystal structure oriented along the *c*-axis. For investigating structure-controlled properties, seed-to-growth solutions concentrations ratio ([S]/[G]) of the synthesis process was varied over six different values. Superhydrophobicity was achieved for all morphologies after 1-dodecanethiol modification, which was highly durable after prolonged UV irradiation. Durability of the ZnO materials under laundry condition was also verified. Variation of the [S]/[G] ratio resulted in a morphological transform from nanorods to needle-like structures in conjunction with a drastic change in the physical and optical properties of the ZnO modified cotton surfaces. Higher [S]/[G] ratios yielded formation of ZnO nanoneedles with high degree of crystallinity and higher aspect ratio compared to nanorods. Increasing [S]/[G] ratio resulted in the amount of ZnO grown on the cotton surface to drop significantly, which also caused a decrease in the surface hydrophobicity and UV absorption. In addition, room temperature photoluminescence measurements revealed that the band gap of ZnO widened and the structural defects were reduced as the morphology changed from nanorods to nanoneedles. A similar trend was observed in the UV−vis absorption of nanorods and nanoneedles, the onset of the latter exhibiting a blue-shift that correlates with the widening of band gap with nanoneedle formation.

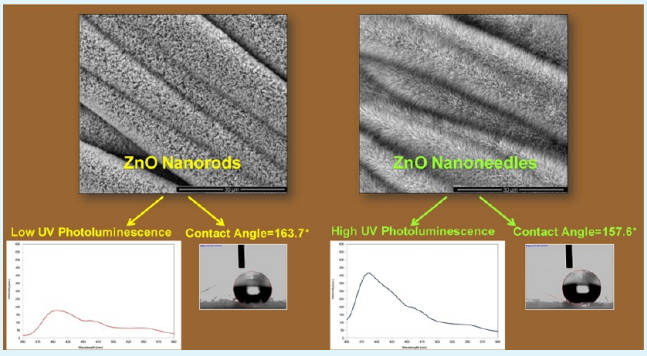

KEYWORDS: *ZnO, structure−activity, nanorods, nanoneedles, hydrophobicity, hydrothermal growth*

INTRODUCTION

Integration of the biocompatible inorganic nanostructures into flexible materials such as plastics, paper, and fabrics will enable design of novel functional materials such as smart clothing with sensing and protection capabilities, wearable electronics, renewable energy systems, and portable and flexible photovoltaic devices.[1−6] Specifically, metal-oxide nanowires could play an important role in the development of these functional materials due to their ease of synthesis, crystallinity, quantum confinement effects, and directional mobility of charge carriers.[7−9] ZnO, a basic II−VI compound semiconductor, is one of the most widely studied metal-oxide semiconductors in the development of conductive electrodes,[10] solar cells,[11−13] protection against UV radiation, wetting, bacterial infection,[14−16] gas sensors,[17] and piezoelectric devices.[18,19] Functionality of ZnO nanowires are ultimately determined by their size, shape, orientation, and crystallinity.[19−22] For example, ZnO nanorods have shown higher photocatalytic activity compared to thin films due to their enhanced surface area-to-volume ratio.[20] In addition, optical properties have also been linked to the size and shape of the solution-bound ZnO naonstructure.[19−22]

Because of the intrinsic anisotropy in the growth rate, resulting ZnO nanostructures take the hexagonal wurtzite structure at ambient conditions. Generally, solution-phase synthesis of ZnO nanowires[21−23] is preferred because of the environmentally friendly, energy efficient, inexpensive, and straightforward nature of the process that can result in the growth of well-aligned, single-crystalline, high-aspect-ratio ZnO nanowires on a wide variety of surfaces,[5,24−26] including fabrics[14,15,27−31] and even paper.[32,33] Homogenous nucleation of solid phases in a solution is not thermodynamically as

Received: April 4, 2013
Accepted: June 12, 2013
Published: June 12, 2013

   dx.doi.org/10.1021/am401229a | ACS Appl. Mater. Interfaces 2013, 5, 6237−6246

favorable as the heterogeneous nucleation onto a surface. Therefore, a process in which substrates were precoated with nanocrystal seeds of the same material as the nucleation sites for controlling the orientation and morphology of the subsequent growth of nanowires have been developed.[34,35] This growth mechanism generally follows a two-step route, which involves a seeding step of a surface and a subsequent solution deposition process, resulting in anisotropic crystal growth of ZnO nanowires.[22,24,34−37]

Growth of uniform and well-aligned ZnO nanowires using the solution-phase method on flexible substrates like cotton poses additional challenges such as weak interaction between the ZnO nanolayers and cotton surface, nonuniform coating, and performance loss with use. A handful of studies on the growth of ZnO structures on cotton surfaces have mostly focused on generation of hydrophobicity and UV protection.[5,14,15,27−30,38,39] Quantitative analysis of the correlation between the process, structure, and resulting physical and optical properties of the ZnO-modified flexible surfaces requires detailed investigation. In this work, we hypothesized that by properly choosing seed-to-growth solutions concentrations ratio ([S]/[G]), it is possible to fine-tune morphology of the ZnO nanowires grown on cotton surfaces and concomitant physical and optical properties such as hydrophobicity, UV absorption, and photoemission. Our strategy was to control the shape, size, and orientation of ZnO nanowires in large arrays directly grown on cotton surfaces by varying [S]/[G] ratios in a solution -phase synthesis.

ZnO nanowires grown on cotton surfaces displayed a significant change in their aspect ratio and morphology as the [S]/[G] ratios varied. Superhydrophobicity was achieved for all morphologies after 1-dodecanethiol modification, which was highly durable after prolonged UV irradiation. Durability of the ZnO nanostructures on the cotton surfaces was also confirmed under vigorous washing conditions. With increasing [S]/[G] ratios, a transformation from nanorod morphology to needle-like (nanoneedles) was observed with accompanying decrease in hydrophobicity and UV-absorption capacity. XRD analysis revealed an increased (002) diffraction peak of nanoneedles, which might be explained by the better orientation of nanoneedles along the *c*-axis. Room temperature photoluminescence (PL) of ZnO nanoneedles in the UV region was enhanced compared to that of nanorods, which can be ascribed to the reduced nonradiative defects in the crystalline structure. In addition, it was evident that the PL and UV emissions of ZnO nanoneedles underwent a blue-shift with an increase in [S]/[G] ratio, which could be due to the widening of the band gap with nanoneedle formation.

EXPERIMENTAL SECTION

2.1. Materials. Bleached desized cotton fabric (#400) was purchased from TestFabrics (West Pittson, PA). Zinc acetate dihydrate ($Zn(CH_3COO)_2.2H_2O$, ACS reagent, ≥ 98%), triethylamine ($(C_2H_5)_3N$ ≥ 99.5%), 1-dodecanethiol ($CH_3(CH_2)_{11}SH$, ≥98.0%), ethanol (CH_3CH_2OH, ACS reagent, ≥99.5% (200 proof), absolute), isopropyl alcohol (C_3H_8O, anhydrous, 99.5%), sodium hydroxide (NaOH, ACS reagent, ≥97.0%, pellets), citric acid ($C_6H_8O_7$, ACS reagent, ≥99.5%), Triton X-100 (laboratory grade nonionic surfactant), zinc nitrate hexahydrate ($Zn(NO_3)_2.6H_2O$, reagent grade 98%), and hexamethylenetetramine ($C_6H_{12}N_4$, ACS reagent, ≥99.0%) were purchased from Sigma-Aldrich.

2.2. Scouring of Cotton Fabric. Before ZnO nanowires were grown, cotton fabric was cut into square swatches (2 cm ×2 cm) and scoured to remove wax, grease, and other finishing chemicals. The scouring solution was prepared by first dissolving 5.0 g of NaOH in 20 mL of deionized water followed by the addition of 1.5 g of Triton X-100 and 0.75 g of citric acid. The resulting solution was then diluted to 500 mL with deionized water. In the scouring process, four cotton swatches were then placed in a 500 mL round-bottom flask containing 200 mL of the scouring solution. The mixture was then stirred at 100 °C for 1 h. At the end of the process, scoured swatches were removed from the solution, rinsed thoroughly with DI water, and dried in air.

2.3. Preparation of ZnO Seed Solution. ZnO seed solution was prepared as follows. First, 100 mM solution of zinc acetate dihydrate was prepared by dissolving 1.10 g (5.0 mmol) in 50.0 mL of isopropyl alcohol. The resulting solution was then stirred vigorously at 85 °C for 15 min. After this time, 700 μL of triethylamine (5.0 mmol) was added dropwise to the stirred solution. The resulting solution, now clear, was stirred at 85 °C for an additional 10 min. After this time, the solution was cooled to room temperature and incubated without stirring for 3 h. The pH of the seed solution was 7.01 (pH meter). The average particle size of the ZnO nanocrystal seed solution was 31.5 ± 10.0 nm, as measured by a Zetatrack (Microtrac) particle size analyzer.† We have used this seed solution up to 2 weeks after its preparation with no discernible change in the final ZnO nanocrystals.

2.4. Preparation of ZnO Growth Solution. Equimolar aqueous solutions of zinc nitrate hexahydrate and hexamethylenetetramine were used to grow ZnO nanorods on cotton swatches. First, a 100 mM solution of hexamethylenetetramine was prepared by dissolving 7.71 g (5.0 mmol) in 550 mL DI water. Once dissolved, 16.4 g of zinc nitrate hexahydrate (5.0 mmol) was added and the resulting solution was stirred for 24 h at room temperature. The final pH of this ZnO growth solution was 6.11 (pH meter). 75.0 mM, 50.0 mM, and 25.0 mM of ZnO growth solutions were also prepared by diluting 100 mM stock solution for investigating the dependence of the structure and properties on the ZnO seed-to-growth solutions concentration ratio.

2.5. Growth of ZnO Nanowires on Cotton Swatches. The scoured cotton swatches were first dip-coated with the ZnO seed solution for 5 min and then rinsed with ethanol. The dip-coated swatches were then suspended from a wire rack,† cured at 120 °C for 1 h in an oven, and then further conditioned in air for 12 h at room temperature. To ensure uniform deposition of ZnO nanowires on cotton surfaces in subsequent steps, the swatches were then immobilized on a glass coverslip using an epoxy glue (LOCTITE stik'n seal ultra, Flextec Technology). The immobilized swatches were then suspended vertically in ∼70 mL of the growth solution and incubated at 95 °C for 8 h in an oven. The container was removed from the oven, cooled to room temperature, and then further incubated at room temperature for 10−12 h. Finally, the swatches were removed from the growth solution, thoroughly rinsed with DI water, and allowed to air-dry at room temperature.

2.6. Hydrophobic Treatment of the ZnO Nanowires Grown on Cotton Swatches. Ten mM of 1-dodecanethiol solution in ethanol was prepared at room temperature. Cotton swatches modified with ZnO nanowires were then immersed in a 20 mL of ethanolic 10 mM 1-dodecanethiol solution for 24 h at room temperature. The samples were then removed, rinsed with ethanol, and cured at 100 °C for 3 h. The samples were then conditioned in air for 12 h. Control samples including unmodified and ZnO seed deposited cotton swatches were also treated in the same manner.

2.7. UV Durability Test of Hydrophobicity. After the hydrophobicity treatment, cotton samples containing ZnO nanorods ([S]/[G] = 1.0) were placed under a UVP Black-Ray B-100AP high intensity UV lamp (100Watt/365 nm/2.5 Amps) with the distance between the sample and the light source of 13 cm. Hydrophobicity of the samples were measured after UV exposure for 3 h.

2.8. Laundry Durability Test of ZnO Modified Cotton Swatches. Real washing conditions were simulated to test the durability of ZnO nanowires on cotton swatches. First, 50 mL of tap water containing 1 wt % of Arm and Hammer laundry Oxi Clean detergent was heated to 90 °C in a round-bottom flask. Cotton swatches modified with ZnO nanorods were then added to the solution and stirred rapidly at 90 °C for 1 h. After this time, the swatches were removed and washed thoroughly with running tap water

to remove detergent. Thermogravimetric analysis were conducted using three samples taken from different spots of the same swatch.

2.9. Characterization. The morphology of the ZnO nanowires grown on cotton swatches was investigated using a JEOL JSM 6060 LV scanning electron microscope (SEM). The samples were coated with 5−10 nm Au layer before the SEM imaging. Elemental analyses of the samples were performed on the SEM system equipped with EDAX TEAM system operating at an accelerating voltage of 20 kV. TEM images were acquired with FEI Tecnai G2 200 kV high-resolution transmission electron microscope. Samples for TEM analyses were prepared as follows. Cotton swatches bearing ZnO nanorods were sonicated in a small beaker containing 40 mL of ethanol for 15 min. Then, HC200 mesh copper grids (Holey carbon film, Electron Microscopy Sciences) was immersed into 20 μL aliquot of this suspension followed by removal slowly. Forceps was used to handle the copper grids which were then air-dried for 2 min for analysis.

Crystal structures were analyzed by X-ray diffraction using a Shimadzu XRD-6100 X-ray Diffractometer with Cu Kα radiation, employing a scanning rate of 0.02° s^{-1} within the range of 2θ = 10−70°, operating at 40 KV and 33 mA (1320 W). Thermogravimetric (TGA) was performed using a Mettler Toledo 851 with a TSO 801RO robotic arm. The samples were heated from 40 to 600 °C at a rate of 10 °C/min under a nitrogen atmosphere at a flow rate of 40 mL/min. UV-transmittance of the samples were studied using a Varian Cary 50 UV−vis Spectrophotometer in wavelength range of 280−480 nm and a scan rate of 300 nm/min. Photoluminescence (PL) spectra were acquired from the aligned ZnO nanowires to reveal their collective optical properties. PL studies were performed at room temperature using a dual-scanning microplate Jasco FP-6500 spectrofluorometer (version 1.08.02) with the Spectra Manager Software using the excitation wavelength at 325 nm. Water contact angles (WCA) were measured using an AST Products VCA Goniometer, which uses a computer-controlled syringe to dispose a 5 μL DI water droplet onto the substrates while calculating the contact angles at room temperature. Hydrophobicity is indicated by the larger water contact angles. The roll-off angles were measured using 40 μL water droplets. The samples were taped onto the rotating table of the instrument before analyses. All contact angles were reported by taking the average of measurements on five random points of each sample surface.

The dimensions of the nanorods were calculated using imaging processing software ImageJ with the scale bar obtained during SEM and TEM acquisition as a reference. At least 5 nanostructures were used in the analysis. The results are tabulated in Table 1.

Table 1. Representative Length and Diameters of the Nanorods and Nanoneedles Generated in This Study

	[S]/[G] (μm)		
	1.0	2.0	4.0
length	1.98 ± 0.07	3.98 ± 0.63	2.72 ± 0.49
diameter	0.172 ± 0.018	N/A	N/A

RESULTS AND DISCUSSION

The optimized two-step solution-phase hydrothermal process for growing ZnO nanowires on cotton surfaces is illustrated in Scheme 1. Six sets of ZnO modified cotton samples were prepared using various seed-to-growth solutions concentrations ([S]/[G]) ratio ranging from 0.50 to 4.0 (Table 2). The process parameters implemented in this study were optimized to obtain uniform arrays of ZnO nanostructures with well-defined morphology. Although several groups previously reported growth of ZnO nanorods on cotton surfaces,[5,14,15,27−30,38] the aforementioned studies were limited with a single [S]/[G] ratio, by which the evaluation of the synthesis parameters on structure and consequent physical and optical properties of the modified surfaces would not be possible. In this work, we report the quantitative correlation between the concentrations of reactants and the structure of the surface-bound ZnO nanowires as well as their physical and optical properties.

Figure 1 presents SEM images of the ZnO nanowires grown on cotton surfaces using six discrete [S]/[G] ratios. Highly uniform, vertically oriented, and dense arrays of ZnO nanowires over a large scale of cotton fibers were successfully achieved. One striking trend that was clearly observed is that the ZnO morphology visibly changes with the increase in the [S]/[G] ratio. We were able to obtain uniform ZnO nanorods with clear-cut hexagonal end planes by keeping the [S]/[G] ratio at 1.3 or lower; above which needle-like structures were obtained. We define nanorods as the structures with well-defined facets and hexagonal cross sections. Nanoneedles, however, have tapered tips and rounded cross sections with higher aspect ratios. The aspect ratio of a shape is defined as the length of the major axis divided by the width of the minor axis. We call nanorods as structures that have aspect ratio less than 20, and nanoneedles with aspect ratio greater than 20.[40] Although the morphology changed from rod to needle-like nanowires, the single crystal wurtzite structure was maintained. Formation of sharp-tipped nanoneedles might be due to the gradual depletion of the growth solution, which yields concentration gradient of Zn from the base to the tip. These results correlates well with the previous reports asserting that the shape of the ZnO particles are very sensitive to the overall concentration of precursors in which the particle diameters became smaller with decreasing concentrations.[36,41] Additionally, Akgun et al.[42] reported the formation of thin and long nanowires with the decrease in the growth solution concentration ratio, which corresponds to increasing [S]/[G] ratio in our work, supporting the validity of our observations.

In earlier works, the effect of temperature, reaction time, solution concentrations, and the type of precursor chemicals and capping agents on the morphology of ZnO nanostructures synthesized using hydrothermal process have been thoroughly investigated and documented.[42−47] The aforementioned studies focused on ZnO nanostructures grown either in solution-phase or on a rigid substrate such as silicon wafer. The systematic study of the process-structure−property relations reported in this study differs from previous investigations significantly since highly flexible, nonuniform, and natural cotton support is used for the growth of well-defined continuous arrays of ZnO nanorods and nanoneedles.

The representative SEM images of the ZnO nanorods that were grown by adopting [S]/[G] ratio of 1.0 are given in Figure 2. It is clearly seen in the cross-sectional SEM views that vertically aligned, uniform, and densely packed arrays of hexagonal ZnO nanorods were successfully achieved over the entire cotton surface with an average diameter of 172 ± 18 nm and length of 1.98 ± 0.07 μm. Figure 3 includes the cross-sectional images of nanoneedles grown maintaining [S]/[G] ratio of 2.0 and 4.0. Each nanorod has a uniform diameter along its entire length which enabled us to calculate its aspect ratio, as seen in Figure 2. However, the needle-like shape of the ZnO nanoneedles with [S]/[G] = 2.0 and 4.0 with large base and sharp tips results in decreasing width along their length (Figure 3). Therefore, aspect ratios for these structures are not available. The results are shown in Table 1.

The effect of synthesis parameters on the morphology of solution-based ZnO nanostructures have been well-established.[48,49] It has been shown that the growth of rodlike

Scheme 1. Schematics of the Two-Step Hydrothermal Process for Growing ZnO Nanowires on Cotton Surfaces

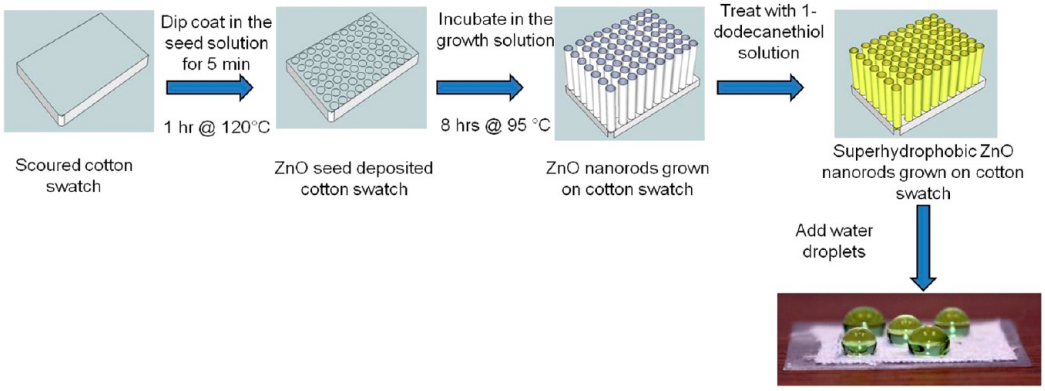

Table 2Variables of the Growth Process, Weight Percentage and Morphology of the ZnO Nanowires Grown on Cotton Surfaces

	sample 1	sample 2	sample 3	sample 4	sample 5	sample 6
[S]/[G]	0.50	0.67	1.0	1.3	2.0	4.0
wt % ZnO nanowires grown on cotton surfaces (TGA)	42.3 (±1.1)	38.4 (±0.3)	37.9 (±0.5)	32.2 (±0.6)	28.4 (±1.8)	16.8 (±0.8)
morphology	nanorods	nanorods	nanorods	nanorods	nanoneedles	nanoneedles

structures are achieved through anisotropic aggregation of the preformed spherical particles, which was also observed in our work (Figure 4). The seeding of the cotton substrate with ZnO nanocrystals was absolutely necessary for the aligned growth of ZnO nanostructures. During the optimization process, we discovered that the seed-to-growth solution concentration ratio is the most important structural control parameter. This might be attributed to the decreasing concentration of available Zn^{2+} in the growth solution per ZnO seed crystal with the increasing [S]/[G] ratio. The concentration gradient of Zn^{2+} results in formation of a needlelike structure with a sharp tip along the *c*-axis and a wide base that starts to nucleate first. This type of behavior has been documented before where smaller seeds yielded thinner ZnO wires and the seed density played an important role in determining the geometric parameters.[47]

The cluster morphology observed in Figure 2 is fairly common and suggests that multiple nanorods frequently grow from a single aggregate of the ZnO nanocrystals deposited onto the cotton surface. Due to the flexible nature of cotton fabric, care needs to be taken specifically during the growth process since unsupported fabrics may curl up, preventing fibers from complete exposure to the solution. In fact, one of the challenges in the synthesis of nanowires on flexible supports is the difficulty in achieving homogeneity. Therefore, we have devised a technique by which cotton swatches were fixed onto glass coverslips with epoxy glue followed by immersion in the growth solution hung by copper wires, which resulted in a uniform and continuous coverage. All characterizations and measurements were carried out with the modified and control samples attached to the glass coverslips.

Chemical composition of the ZnO nanowires grown on cotton surfaces was verified by energy dispersive X-ray (EDX) spectroscopy. Panels a and b in Figure 5 display EDX micrographs of an unmodified and ZnO nanorods modified cotton samples ([S]/[G] = 1.0). As seen in Figure 5, the scoured cotton swatch does not contain any contaminants, indicated by the sole presence of carbon (C) and oxygen (O) atoms. Figure 5b reveals that the ZnO modified cotton sample contains only zinc (Zn), carbon, and oxygen atoms, indicating high purity of the grown ZnO nanorods within the detection limit of EDX. EDX micrographs of the other five samples can be found in the Supporting Information.

Compositional ZnO content of the modified cotton samples was further assessed by thermogravimetric analysis (TGA). Figure 6 presents the representative thermograms of the unmodified, seed layer deposited, and ZnO nanorod modified cotton samples ([S]/[G] = 1.0). Up to 50 °C, most of the weight loss is due to the desorption of the solvent and/or water. Therefore, the weight losses were calculated by taking the weight of the sample at 50 °C as the starting point. The weight of all samples was observed to drop sharply between 300 and 350 °C. Unmodified and seed-layer deposited cotton samples start to thermally decompose around 250 °C, and the total decomposition of unmodified cotton is completed around 540 °C. The amount of ZnO seed nanocrystals and nanorods after the seeding and the growth step was calculated by the weight loss of the samples at the end of the heating cycle, as 7.06 (±1.02) wt % and 37.9 (±0.5) wt %, respectively. The thermograms of other five samples can be found in the Supporting Information.

The most striking result of the TGA experiments is the close linear correlation between the amount of ZnO nanowires grown on cotton swatches and the seed-to-growth solutions concentrations ratio ([S]/[G]) used to grow them. The first order linear regression curve versus [S]/[G] ratios used in this study is presented in Figure 7. The amount of ZnO grown on cotton swatches drops markedly as the [S]/[G] ratios increase. There is a close linear correlation between the amount of ZnO and [S]/[G] ratio with an R^2 (coefficient of determination) value of 0.97. This observation would be very useful in establishing a quantitative relationship between the morphology of ZnO nanowires and the seed-to-growth solutions concentrations ratio and could enable designs of ZnO nanowire-modified surfaces with desired physical and optical properties using the reported procedure.

Real washing conditions were simulated to test the durability of ZnO nanowires on cotton swatches generated by our optimized method. The ZnO nanorods on the cotton surfaces were found to be highly durable: after washing with commercial laundry detergent in water at 90 °C for one hour, no

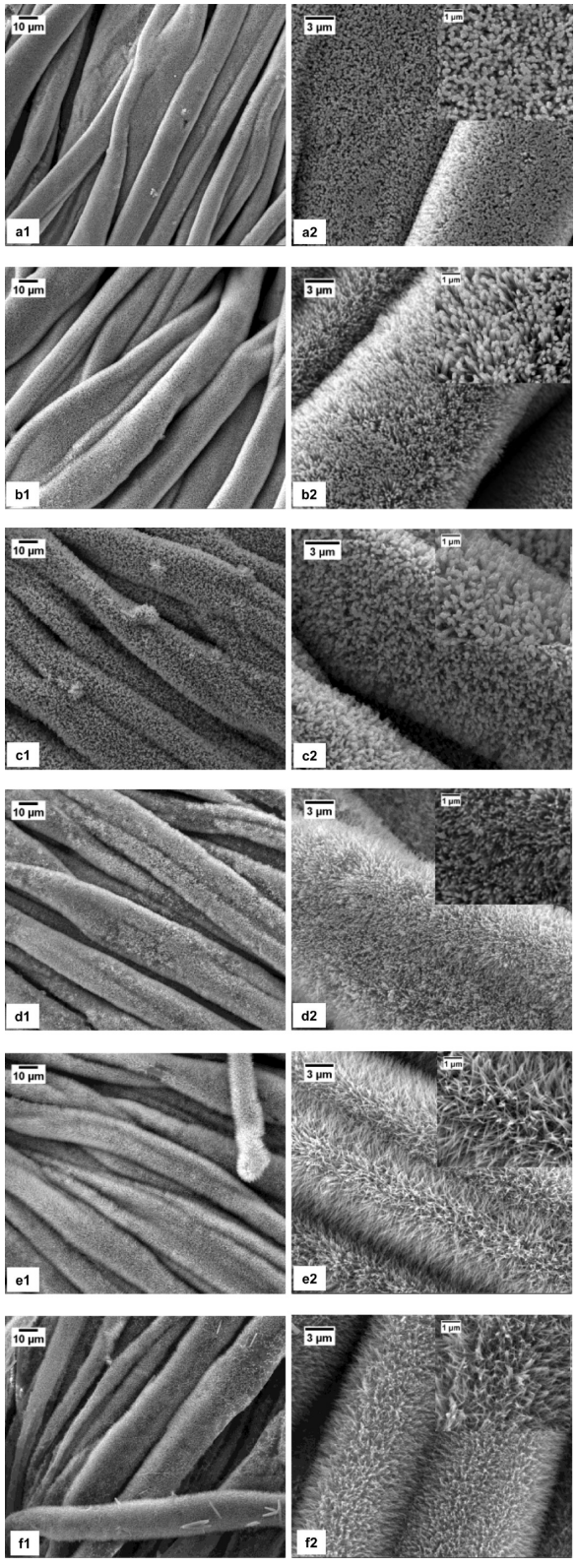

Figure 1. SEM images of the (a–d) ZnO nanorods and (e, f) nanoneedles grown on cotton surfaces with different magnifications (a1, a2) [S]/[G] = 0.50, (b1, b2) [S]/[G] = 0.67, (c1, c2) [S]/[G] = 1.00, (d1, d2) [S]/[G] = 1.33, (e1, e2) [S]/[G] = 2.00, and (f1, f2) [S]/[G] = 4.00.

statistically significant change of the structure and amount of ZnO nanowires was observed by SEM investigation or thermogravimetric analysis. The average loading of the ZnO

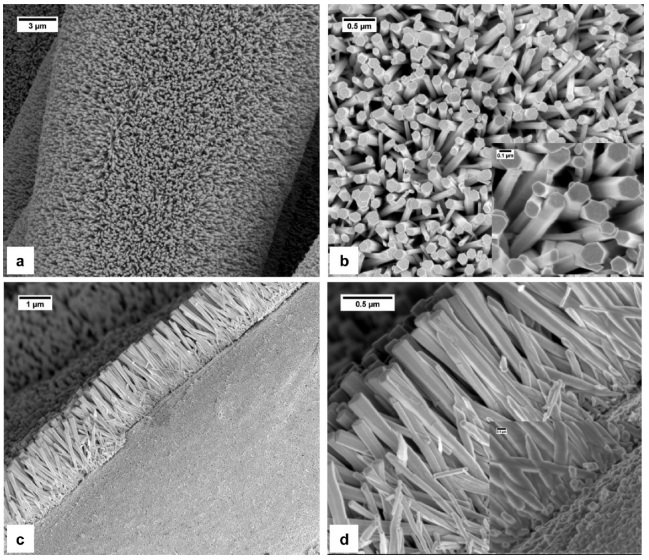

Figure 2. SEM images of (a, b) the ZnO nanorods grown on cotton surface at different magnifications, ([S]/[G] = 1.0) (c, d) cross-sectional images of the ZnO nanorods grown on cotton surface at different magnifications ([S]/[G] = 1.0).

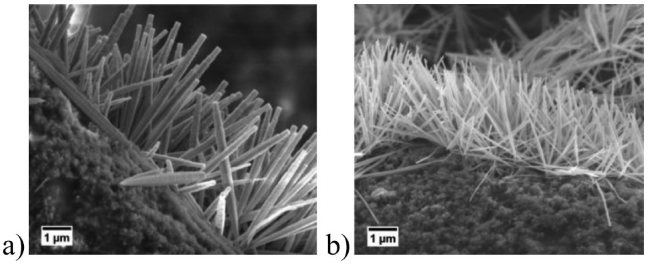

Figure 3. Cross-sectional SEM images of the ZnO nanoneedles grown on cotton surfaces (a) [S]/[G] = 2.00, and (b) [S]/[G] = 4.00.

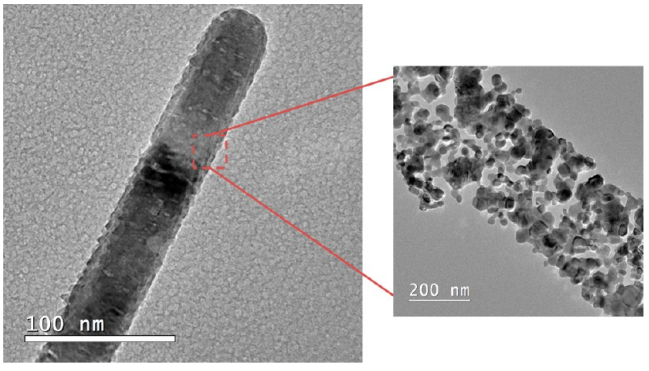

Figure 4. TEM images of nanorods with higher magnification showing the aggregation of preformed ZnO spherical particles during the anisotropic growth of ZnO nanowires.

on cotton swatches before and after washing were found as 21.7 ± 1.5 wt % and 22.3 ± 1.5 wt %, respectively. The results of thermogravimetric analysis indicate that there is no statistical difference in ZnO content before and after detergent washing and the ZnO nanorods were durable under the detergent washing conditions. Comparison of SEM images before and after washing (Figure 8) was also consistent with little to no change in the ZnO content and morphology. These experi-

dx.doi.org/10.1021/am401229a | ACS Appl. Mater. Interfaces 2013, 5, 6237–6246

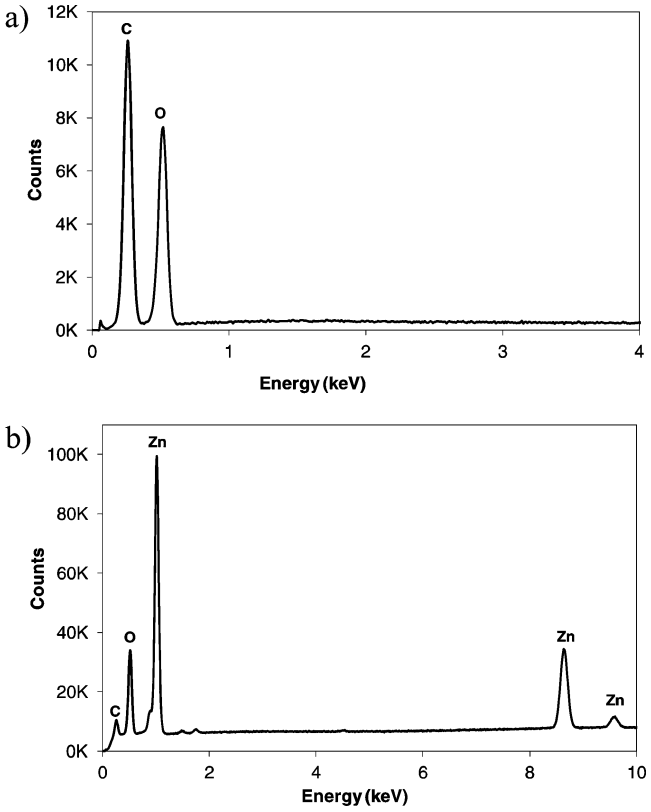

Figure 5. EDX micrographs of (a) unmodified scoured cotton, and (b) ZnO nanorods grown on cotton sample ([S]/[G] = 1.0).

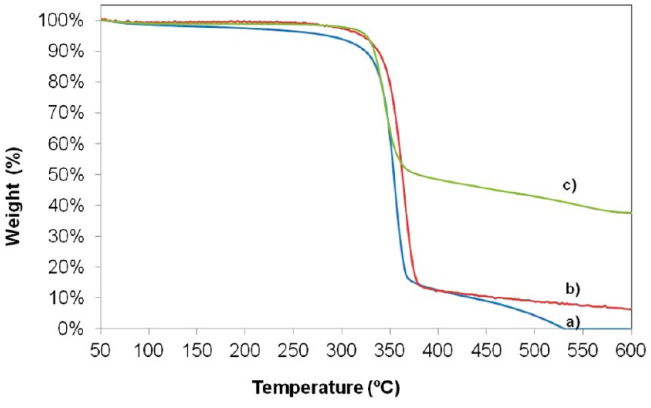

Figure 6. Thermograms of (a) unmodified scoured cotton, (b) ZnO seed-deposited cotton, and (c) ZnO nanorods grown cotton samples ([S]/[G] = 1.0).

ments demonstrate the durability of the ZnO nanowires grown on cotton swatches.

The degree of crystallinity of the cotton-bound ZnO nanowires was studied by X-ray diffraction analysis. Figure 9 presents representative XRD patterns of unmodified and ZnO nanorods grown cotton samples with [S]/[G] = 1.0 and [S]/[G] = 2.0. The peaks at 2θ values of 15.2, 16.7, and 23.1° corresponding to (101), (10$\bar{1}$), (002) planes, respectively, are the diffraction peaks of cotton fiber (cellulose I structure) (JCPDS. No. 03−0226).[40] Six reflection peaks appeared at 2θ values of 31.9° (100), 34.6° (002), 36.5° (101), 47.7° (102), 56.8° (110), 63.1° (103), and all the diffraction peaks could be indexed as the hexagonal wurtzite structure of ZnO, which were consistent with the values in the standard card (JCPDS 36−1451). The symmetrical narrow full width at half-maximum (fwhm) of the ZnO peaks show that ZnO nanowires are well crystallized.

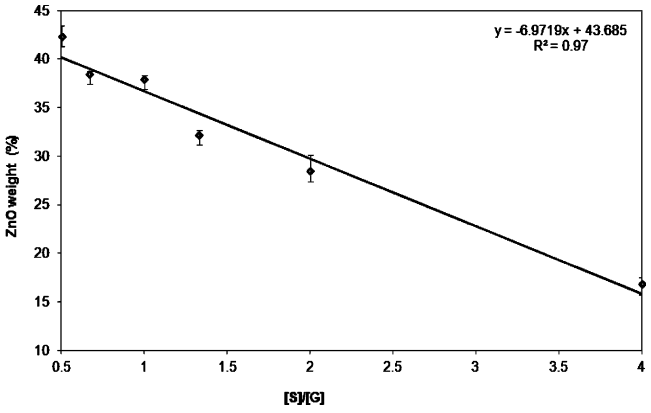

Figure 7. Amount of ZnO (wt %) nanowires grown on cotton surfaces using various [S]/[G] ratios. Solid line indicates the regression analysis of the entire data.

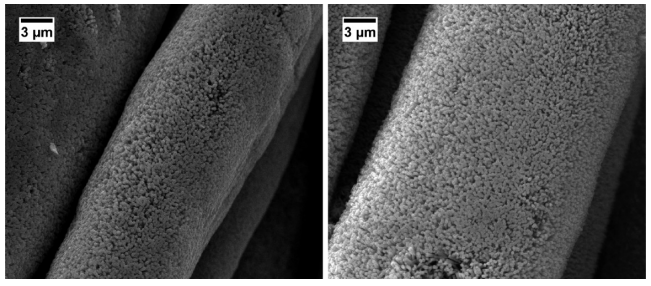

Figure 8. SEM images of ZnO nanorods ([S]/[G] = 1.0) grown on cotton surfaces (a) before and (b) after washing for 1 h at 90 °C in tap water containing 1 wt % commercial laundry detergent.

The wurtzite structure is the thermodynamically most feasible form of the hydrothermal anisotropic growth owing to the presence of polar and nonpolar surfaces, with a natural tendency to minimize polar surface in order to reduce surface energy.[32] No diffraction peaks from any other phases are found, confirming that the only single-phase hexagonal ZnO is present. The enhanced (002) diffraction peaks in Figure 9 b and c indicate preferential growth along the *c*-axis for nanorods and nanoneedles. In many previous works, calcination at higher temperatures (≥300 °C) has been required to achieve single crystal ZnO nanostructures. However, we achieved a high degree of crystallinity using relatively low temperature hydrothermal growth technique on a flexible surface notoriously difficult to work with which is comparable, in terms of quality, to those obtained using high-temperature methods and/or calcination. Additional XRD patterns of selected samples can be found in the Supporting Information.

The structural dependence of the optical properties of ZnO nanowires was studied by photoluminescence (PL) measurements under 325 nm excitation light source at room temperature over a wavelength range of 350−600 nm. PL spectrum of the ZnO nanowires grown on cotton swatches are given in Figure 10. Typical PL spectra of n-type ZnO crystal (E_g = 3.37 eV) has a UV near band-edge emission and a visible deep-level emission peaks, where the latter is related to structure defects such as oxygen vacancies (O_v) and interstitials (O_i), and zinc vacancies (V_{Zn}) and interstitials (ZnO_i).[50,51] The PL emission peak at 377 nm in the UV region corresponds to

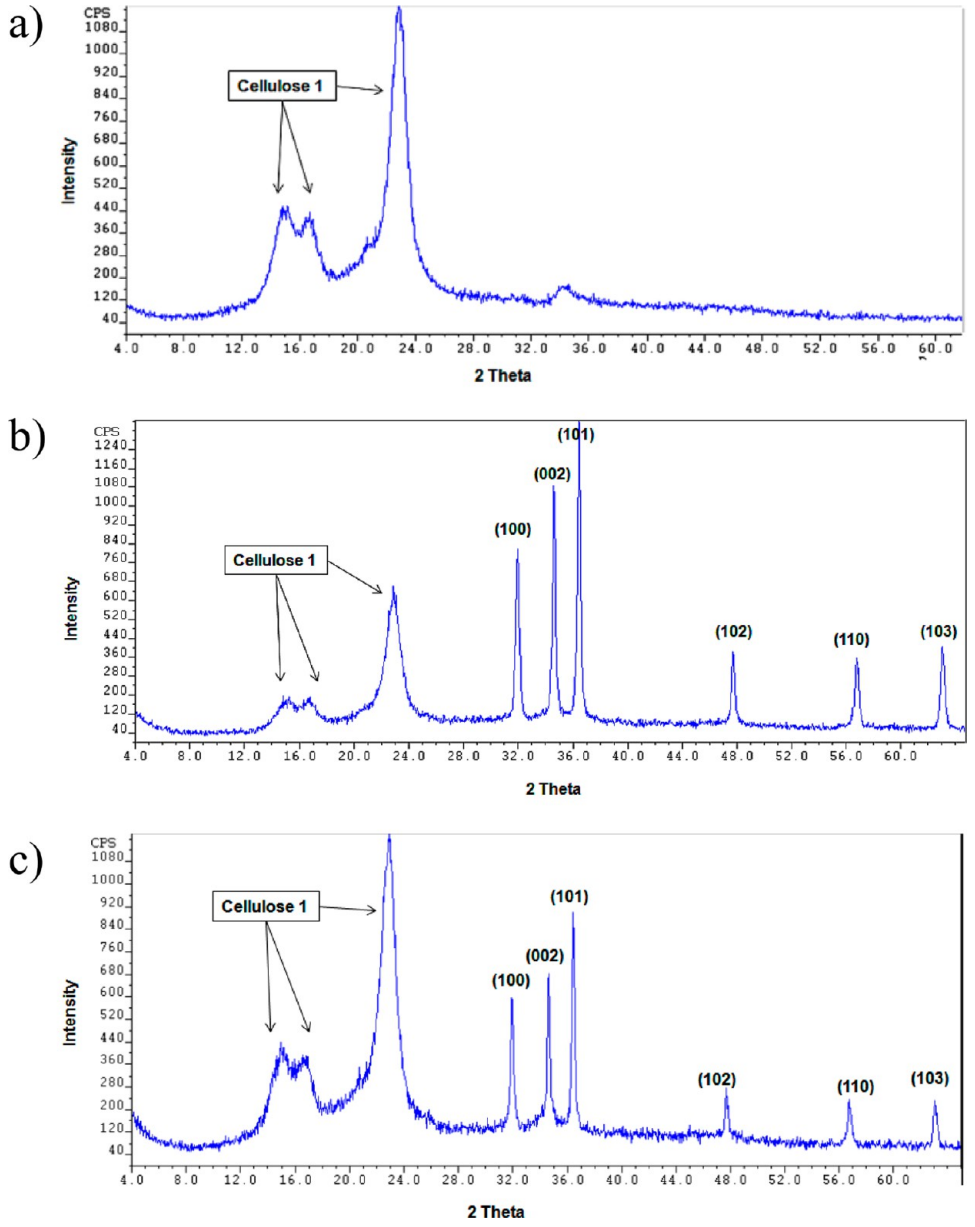

Figure 9. Indexed XRD patterns of (a) unmodified cotton and (b) ZnO nanorods grown cotton sample ([S]/[G] = 1.0), and (c) ZnO nanoneedles grown cotton sample ([S]/[G] = 2.0).

recombination of charge carriers between the conduction and valence bands of ZnO crystal. In general, the PL spectrum of powder or polycrystalline thin film of ZnO shows much stronger visible emissions than UV emissions, whereas the epitaxial thin films on lattice-matched single-crystalline substrates show weaker visible emissions because of the reduced structural defects, as is the case in this study. As evident in Figure 10, ZnO nanorods and nanoneedles all have significantly lower visible deep-level emissions compared to UV near band-edge emissions, indicating that the ZnO nanorods and nanoneedles are almost defect-free and of high quality. The high UV-to-Visible emission ratio indicates a good crystal quality of the nanowires, i.e. a low density of surface defects. The ratio of the UV near band-edge to the visible deep level emission increased markedly with increasing [S]/[G] ratio, suggesting the presence of fewer defects and enhanced crystal quality of ZnO nanoneedles compared to nanorods.

There is a large blue shift of about 15 nm in the PL emission peak in the UV region with increasing [S]/[G] ratio, indicating a widening of the band gap with nanoneedles formation. The observed morphology-dependent shift in the peak positions of the band-edge recombination might be attributed to different native defect concentrations originating from surface/volume ratio differences. Our observation corroborates well with the previous report showing a band gap increase with the reduced size for colloidal solutions by Greene et al.[37] In addition, comparable findings, where the UV emission peaks also moved toward higher energy with decreasing ZnO nanorod diameters were reported in the literature.[52,53]

UV−vis transmittance spectroscopy is another technique for further studying the structural effect on the optical properties of the surface-bound ZnO nanowires. ZnO strongly absorbs in the UV region due to its direct band gap of 3.37 eV.[15−18] Figure 11 depicts the representative transmittance spectra of unmodified, ZnO nanoneedles, and nanorod-modified cotton samples over

dx.doi.org/10.1021/am401229a | ACS Appl. Mater. Interfaces 2013, 5, 6237−6246

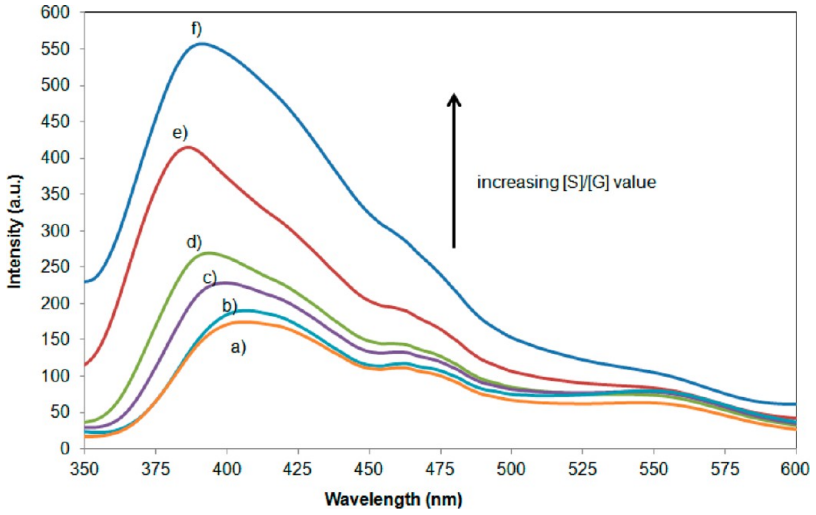

Figure 10. Photoluminescence spectra of ZnO nanowires grown on cotton surfaces with (a) [S]/[G] = 0.50, (b) [S]/[G] = 0.67, (c) [S]/[G] = 1.00, (d) [S]/[G] = 1.33, (e) [S]/[G] = 2.00, and (f) [S]/[G] = 4.00.

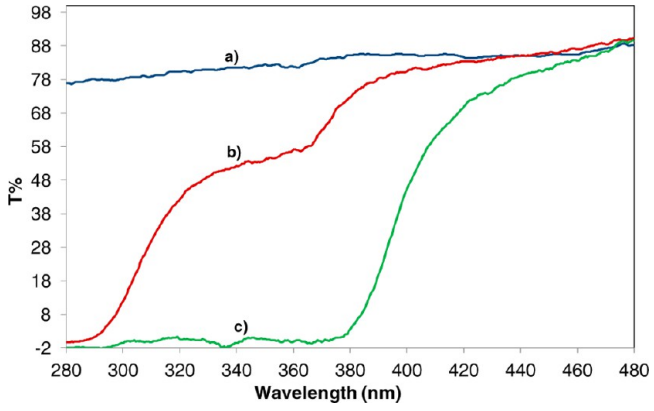

Figure 11. UV−vis transmittance spectra of (a) unmodified cotton, (b) ZnO nanoneedles grown cotton ([S]/[G] = 4.00), and (c) ZnO nanorods grown cotton samples ([S]/[G] = 1.00).

the wavelength range of 280−480 nm. Untreated cotton absorbs only 22% of the radiation over the entire region. The presence of nanorods and nanoneedles significantly increase the absorption and scattering of the irradiation, nanorods being more effective than nanoneedles, which is not surprising because the amount of ZnO arrays that can absorb the incoming photons is much higher (37.9 ± 0.5 wt %) compared to that of nanoneedles (16.8 ± 0.8 wt %). ZnO nanorods have absorption onset at 378 nm (3.28 eV), whereas the absorption edge shifts toward blue about 13 nm (365 nm, 3.39 eV) with nanoneedle formation. The absorption onset of ZnO structures is attributed to the interband transition. UV−vis spectra of nanoneedles exhibiting a blue shift of the absorption onset provides further indication of the widening band gap and in agreement with the PL observations. These results suggest that the degree of crystallinity is significantly improved with the nanoneedle formation. UV−vis transmission spectra of the remaining samples can be found in the Supporting Information.

To test a possible interference of the epoxy glue used to secure cotton swatches with the spectroscopic analyses of ZnO nanowires, we recorded the transmittance and photoluminescence spectra of epoxy containing glass coverslips as a control. We observed that the presence of epoxy did not have any significant contributions to the photoluminescence or UV−vis transmittance of the ZnO containing cotton samples. Optical UV absorption onset of glass coverslip was recorded around 320 nm, which is far below the absorption onsets of ZnO nanorods and nanoneedles. Consequently, we can confidently conclude that there is no optical interference originating from the glass coverslip or epoxy glue in these experiments.

Surface wettability is determined by the combined effect of surface chemical composition and morphology. Highly textured arrays of ZnO in combination with chemical modification have been shown to exhibit superhydrophobic behavior.[5,14,15,27−30,38,39] In addition, superhydrophobic cotton fabrics modified with ZnO nanorods have been prepared by a combination of SiO_2 nanoparticle deposition and organosilane modification.[38,39] In our work, superhydrophobicity was achieved for all samples after the treatment with 10 mM ethanolic 1-dodecanethiol solution. Surface wettability was evaluated by measuring the static water contact angles (WCA) of 5 μL water droplets on five different locations on the surface of the samples. Unmodified, ZnO seed-deposited, and ZnO nanowire-grown cotton samples were all initially hydrophilic. A scoured cotton swatch was also treated with 1-dodecanethiol for comparison purposes which also was determined to be hydrophilic, despite a delayed absorption rate. However, ZnO seed-deposited cotton swatches after the hydrophobicity treatment displayed WCA of 137.80° ± 1.21. Figure 12 shows that the WCA and hence hydrophobicity of the prepared samples is decreasing steadily with increasing [S]/[G] ratios, suggesting that the nanoneedles modified surfaces are less hydrophobic compared to those of nanorods. The UV durability of the ZnO modification on cotton substrates were also tested by exposing samples to UV irradiation over 3 h. At the end of the specified time, the water contact angles were measured. The samples maintained their superhydrophobicity after the UV exposure, indicating that the hydrophobic coating of 1-dodecanethiol is durable against UV irradiation for at least three hours.

The roll-off angle is also a useful parameter for evaluating surface wetting that gives the maximum tilt angle that can be achieved before a drop is released. As listed in Table 3, roll-off angles increased significantly from nanorods to nanoneedles, indicating that the droplets stick to the less hydrophobic nanoneedles surface. Contact angle hysteresis, the difference

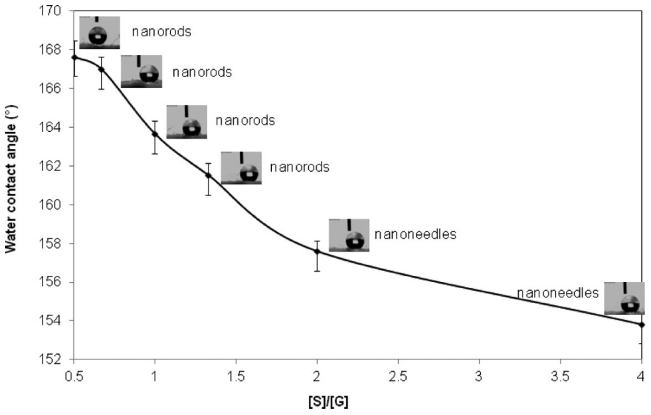

Figure 12. Variations in the water contact angles of the ZnO nanowires grown on cotton surfaces treated with 1-dodecanethiol as a function of [S]/[G].

Table 3. Wettability Analysis of ZnO Nanowire-Modified Cotton Surfaces

[S]/[G]	advancing WCA (deg)	receding WCA (deg)	contact angle hysteresis (deg)	roll-off angle (deg)
0.50	167.64 (±0.83)	167.30 (±0.88)	0.34	11.10
0.67	167.00 (±0.63)	166.22 (±0.83)	0.78	13.00
1.00	163.66 (±0.68)	163.26 (±0.54)	0.40	16.40
1.33	161.52 (±0.65)	161.30 (±0.63)	0.22	19.10
2.00	157.60 (±0.56)	156.62 (±0.74)	0.98	21.10
4.00	153.82 (±0.68)	153.32 (±0.86)	0.50	30.50

between advancing and receding contact angles, characterizes surface heterogeneity. The contact angle hysteresis as a function of [S]/[G] ratios are listed in Table 3. For all samples, very small contact angle hysteresis, less than 1°, were observed, confirming that highly uniform and homogeneous superhydrophobic array of ZnO nanowires were successfully grown on cotton surfaces using the reported hydrothermal growth technique.

CONCLUSION

In conclusion, we have successfully grown ZnO nanorods and nanoneedles on cotton surfaces by varying the seed-to-growth solutions concentrations ratio ([S]/[G]) in a two-step optimized hydrothermal process at a relatively low temperature in aqueous solution. This multifunctional cotton textile has a high UV absorbency, superhydrophobicity that is durable under UV irradiation, and durability under harsh washing conditions. Our optimized growth process, which accurately controls the morphology of the synthesized ZnO nanostructures, is straightforward, cost-effective, environmentally benign, reproducible, scalable, and can be applied to variety of surfaces such as nylon[54] and electrospun nonwoven surfaces of cellulosic polymers[55] and amides.[26] We observed that the increasing [S]/[G] ratio leads to a transformation of ZnO nanostructures from rodlike to needlelike morphology with high aspect ratios. A quantitative correlation was established between [S]/[G] ratio and the amount of ZnO nanowires grown on a cotton substrate. The morphology of the ZnO nanowires has a significant impact on the physical and optical properties of the modified cotton surfaces. Photoluminescence in the deep UV region increase with increasing [S]/[G] ratio, indicating that nanoneedles have fewer nonradiative transitions between excitonic states. A blueshift both in the deep UV region emission and absorption onset of ZnO nanoneedles were observed, which was attributed to the decreasing structural defects and widening band gap, respectively. UV−vis absorption, however, decreases with increasing [S]/[G] ratio.

Subsequent modification with alkyl chains rendered the cotton surface with ZnO nanowires superhydrophobic characterized by the advancing/receding water contact angle. Rodlike arrays exhibited the highest water contact angles, which decrease with the nanoneedle formation. This observation is not surprising given the fact that the amount of nanoneedles on the surface is lower compared to that of nanorods. In addition, the nanoneedles tend to bend because of their high aspect ratio as seen in SEM images, which might alter the roughness of the surface and the interaction with the water droplet. The contact angle hysteresis of all of the samples with various [S]/[G] ratio were found to be very low, indicating the formation of uniform arrays of ZnO nanowires on cotton surfaces. It is now possible to be able to apply the relations that have been laid out in this study to find possible structures or process settings resulting in a certain combination of desired properties.

As a result, quantitative roadmap for guiding the synthesis of ZnO nanowires that will possess targeted crystallinity, hydrophobicity, photoluminescence, and UV absorption was obtained. Given that the performance of nanomaterials depends on their size, shape, and orientation, a clear understanding of the quantitative correlation between the morphology and the physical and optical properties is critically important for the development of nanostructured functional materials and devices. For instance, higher photoefficiency and surface conductivity are anticipated in view of the developed thin and continuous arrays of ZnO nanowires combined with directional mobility of charge carriers due to the quantum confinement effect. More importantly, ZnO nanoneedles with a high UV-absorption capacity, visible transparency, and widened band gap hold great promise for the development of wearable and/or flexible photovoltaics, transparent conductors, and protective clothing while all exhibiting self-cleaning properties.

ASSOCIATED CONTENT

Supporting Information

Size distribution of the ZnO nanocrystals in the seed solution; images of the experimental setup; EDX micrographs and elemental compositions; control photoluminescence and UV−vis transmission experiments of the epoxy containing glass coverslip, thermograms, XRD patterns, and UV−vis transmittance spectra of all the samples prepared; images of 5 μL of water droplets used to determine the advancing and receding contact angles; and a video showing the hydrophobicity of the ZnO-modified cotton. This material is available free of charge via the Internet at http://pubs.acs.org/.

AUTHOR INFORMATION

Corresponding Author

*E-mail: ruya-ozer@utulsa.edu.

Author Contributions

The manuscript was written through contributions of all authors. All authors have given approval to the final version of the manuscript.

Notes

The authors declare no competing financial interest.

■ ACKNOWLEDGMENTS

We thank The Department of Chemistry & Biochemistry at The University of Tulsa for its support. We greatly appreciate the financial support from The University of Tulsa Institute of Nanotechnology, Bellwether Fellowship, TU Student Research Grants Program, and the Faculty Development Summer Fellowship and Research Programs for financial support. Paige Johnson, Rick Portman, and Dr. Winton Cornell are acknowledged for technical assistance. We also thank Dr. Justin Chalker for valuable discussions.

■ REFERENCES

(1) Ko, H.; Kapadia, R.; Takei, K.; Takahashi, T.; Zhang, X.; Javey, A. *Nanotechnology* **2012**, *23*, 344001.
(2) Wagner, S.; Bauer, S. *MRS Bull.* **2012**, *37*, 207−213.
(3) Cherenack, K.; Van Pieterson, L. *J. Appl. Phys.* **2012**, *112*, 091301.
(4) Yang, P.; Wu, Y.; Yan, H.; Huang, M.; Messer, B.; Song, J. H.; Yang, P. *Chem.—Eur. J.* **2002**, 1260−1268.
(5) Lee, M.; Kwak, G.; Yong, K. *ACS Appl. Mater.Interfaces* **2011**, *3*, 3350−3356.
(6) Rogers, J. A; Someya, T.; Huang, Y. *Science* **2010**, *327*, 1603−1607.
(7) Lieber, C. M. *MRS Bull.* **2011**, *36*, 1052−1064.
(8) Tian, B.; Lieber, C. M. *Pure Appl. Chem.* **2011**, *83*, 2153−2169.
(9) Xiong, Q.; Grimes, C. a.; Zacharias, M.; Morral, A. F. I.; Hiruma, K.; Shen, G. *J. Nanotech.* **2012**, special issue.
(10) Scott, R. C.; Leedy, K. D.; Bayraktaroglu, B.; Look, D. C.; Zhang, Y.-H. *Appl. Phys. Lett.* **2010**, *97*, 072113.
(11) Ravirajan, P.; Peiró, A. *J. Phys.Chem.B* **2006**, 7635−7639.
(12) Thambidurai, M.; Muthukumaramsy, N.; Velauthapillai, D.; Arul, N.; Agilan, S.; Balasundaraprabhu, R. *J. Mater. Sci. Mater. Electron.* **2011**, *22*, 1662−1666.
(13) Ko, S.; Lee, D.; Kang, H.; Nam, K.; Yeo, J. *Nano Lett.* **2011**, *11*, 666−671.
(14) Qi, G.; Zhang, H.; Yuan, Z. *Appl. Surf. Sci.* **2011**, *258*, 662−667.
(15) Xu, B.; Cai, Z. *J. Appl. Polym. Sci.* **2008**, *108*, 3781−3786.
(16) Athauda, T. J.; Ozer, R. R.; Chalker, J. M. *RSC Adv.* **2013**, *3*, 10662−10665.
(17) Liu, J.; Wu, W.; Bai, S.; Qin, Y. *ACS Appl. Mater. Interfaces* **2011**, *3*, 4197−200.
(18) Wang, Z. *MRS Bull.* **2012**, *37*, 814−827.
(19) Ahmad, M.; Zhu, J. *J. Mater. Chem.* **2010**, *21*, 599−614.
(20) Baruah, S.; Mahmood, M. A.; Myint, M. T. Z.; Bora, T.; Dutta, J. *Beilstein J. Nanotechnol.* **2010**, *1*, 14−20.
(21) Xu, S.; Wang, Z. L. *Nano Res.* **2011**, *4*, 1013−1098.
(22) Baruah, S.; Dutta, J. *Sci. Technol. Adv. Mater.* **2009**, *10*, 013001.
(23) Hari, P.; Spencer, D. *Phys. Status Solidi (C)* **2009**, *6*, S150−S153.
(24) Vayssieres, L.; Keis, K.; Lindquist, S.; Hagfeldt, A. *J. Phys. Chem. B* **2001**, *28*, 3350−3352.
(25) Baruah, S.; Thanachayanont, C.; Dutta, J. *Sci. Technol. Adv. Mater.* **2008**, *9*, 025009.
(26) Athauda, T. J.; Butt, U.; Ozer, R. R. *MRS Commun.* **2013**, *3*, 51−55.
(27) Wang, R.; Xin, J.; Tao, X.; Daoud, W. *Chem. Phys. Lett.* **2004**, *398*, 250−255.
(28) Xu, B.; Cai, Z. *Appl. Surf. Sci.* **2008**, *254*, 5899−5904.
(29) Wang, L.; Zhang, X.; Li, B.; Sun, P.; Yang, J.; Xu, H.; Liu, Y. *ACS Appl. Mater. Interfaces* **2011**, *3*, 1277−1281.
(30) Ates, E. S.; Unalan, H. E. *Thin Solid Films* **2012**, *520*, 4658−4661.
(31) Zhou, Z.; Zhao, Y.; Cai, Z. *Appl. Surf. Sci.* **2010**, *256*, 4724−4728.
(32) Baruah, S.; Jaisai, M. *Sci. Tech. Adv. Mater.* **2010**, 055002.
(33) Manekkathodi, A.; Lu, M. *Adv. Mater.* **2010**, *22*, 4059−4063.
(34) Greene, L. E.; Law, M.; Goldberger, J.; Kim, F.; Johnson, J. C.; Zhang, Y.; Saykally, R. J.; Yang, P. *Angew. Chem., Int. Ed.* **2003**, *42*, 3031−3034.
(35) Greene, L. E.; Law, M.; Tan, D. H.; Montano, M.; Goldberger, J.; Somorjai, G.; Yang, P. *Nano Lett.* **2005**, *5*, 1231−1236.
(36) Vayssieres, L. *Adv. Mater.* **2003**, *15*, 464−466.
(37) Greene, L.; Yuhas, B.; Law, M. *Inorg. Chem.* **2006**, *45*, 4977−4984.
(38) Xu, B.; Cai, Z.; Wang, W.; Ge, F. *Surf. Coat. Technol.* **2010**, *204*, 1556−1561.
(39) Wang, L.; Zhang, X.; Fu, Y.; Li, B.; Liu, Y. *Langmuir* **2009**, *25*, 13619−13624.
(40) Murphy, C. J.; Jana, N. R. *Adv. Mater.* **2002**, *14*, 80−82.
(41) Pacholski, C.; Kornowski, A.; Weller, H. *Angew. Chem., Int. Ed.* **2002**, *0*, 1188−1191.
(42) Akgun, M. C.; Kalay, Y. E.; Unalan, H. E. *J. Mater. Res.* **2012**, 1445−1451.
(43) Wang, S.-F.; Tseng, T.-Y.; Wang, Y.-R.; Wang, C.-Y.; Lu, H.-C.; Shih, W.-L. *Int. J. Appl. Ceram. Tech.* **2008**, *5*, 419−429.
(44) Cheng, B.; Samulski, E. T. *Chem. Commun.* **2004**, 986−987.
(45) Liu, Y.; Kang, Z. H.; Chen, Z. H.; Shafiq, I.; Zapien, J. A.; Bello, I. *Cryst. Growth Des.* **2009**, *9*, 3222−3227.
(46) Lee, Y.-J.; Sounart, T. L.; Liu, J.; Spoerke, E. D.; McKenzie, B. B.; Hsu, J. W. P.; Voigt, J. A. *Cryst. Growth Des.* **2008**, *8*, 2036−2040.
(47) Zhao, X.; Lee, J. Y.; Kim, C.-R.; Heo, J.; Shin, C. M.; Leem, J.-Y.; Ryu, H.; Chang, J.-H.; Lee, H. C.; Jung, W.-G.; Son, C.-S.; Shin, B. C.; Lee, W.-J.; Tan, S. T.; Zhao, J.; Sun, X. *Physica E* **2009**, *41*, 1423−1426.
(48) Govender, K.; Boyle, D. S.; Kenway, P. B.; O'Brien, P. *J. Mater. Chem.* **2004**, 2575−2591.
(49) Zheng, Y.; Chen, C.; Zhan, Y.; Lin, X.; Zheng, Q.; Wei, K.; Zhu, J.; Zhu, Y. *Inorg. Chem.* **2007**, *46*, 6675−82.
(50) Liu, Z.; Ong, C.; Yu, T.; Shen, Z. *Appl. Phys. Lett.* **2006**, *88*, 053110.
(51) Vempati, S.; Mitra, J.; Dawson, P. *Nano.Res. Lett.* **2012**, *7*, 470−479.
(52) Chen, C.-W.; Chen, K.-H.; Shen, C.-H.; Ganguly, A.; Chen, L.-C.; Wu, J.-J.; Wen, H.-I.; Pong, W.-F. *Appl. Phys. Lett.* **2006**, *88*, 241905.
(53) Yang, Y. H.; Chen, X. Y.; Feng, Y.; Yang, G. W. *Nano Lett.* **2007**, *7*, 3879−3883.
(54) Athauda, T. J.; Ozer, R. R. *Cryst. Growth Des* **2013**, *13*, 2680−2686.
(55) Athauda, T. J.; Butt, U.; Harikumar, P.; Ozer, R. R. *MRS Proc.* **2012**, *1439*, 39−44.